Available online at www.sciencedirect.com
ScienceDirect
Advances in Space Research 43 (2009) 253–264
ADVANCES IN SPACE RESEARCH (a COSPAR publication)
www.elsevier.com/locate/asr

Wave emissions at half electron gyroharmonics in the equatorial plasmasphere region: CLUSTER observations and statistics

F. El-Lemdani Mazouz [a,*], J.L. Rauch [a], P.M.E. Décréau [a], J.G. Trotignon [a], X. Vallières [a], F. Darrouzet [b], P. Canu [c], X. Suraud [a]

[a] Laboratoire de Physique et de Chimie de l'Environnement (LPCE), 3A Avenue de la recherche Scientifique, 45071 Orléans Cedex 02, France
[b] Belgian Institute for Space Aeronomy (IASB-BIRA), 3 Avenue Circulaire, 1180 Brussels, Belgium
[c] Centre d'études des Environnements Terrestres et Planétaires (CETP), 10–12 Avenue de l'Europe, 78140 Vélizy-Villacoublay, France

Received 16 November 2007; received in revised form 26 May 2008; accepted 6 June 2008

Abstract

Intense $(n + 1/2)\, f_{ce}$ emissions are a common phenomenon observed in the terrestrial inner magnetosphere. One of their interests is their possible effect in the pitch angle scattering of plasmasheet keV-electron, leading to diffuse auroras. In this paper, we present CLUSTER's point of view about this topic, in the equatorial region of the plasmasphere, via a statistical study using 3 years of data. Spectral characteristics of these waves, which represent an important clue concerning their generation mechanism, are obtained using WHISPER data near perigee. Details on the wave spectral signature are shown in an event study, in particular their splitting in fine frequency bands. The orbit configuration of the four spacecraft offers a complete sampling on all MLT sectors. A higher occurrence rate of the emissions in the dawn sector and their confinement to the geomagnetic equator, pointed out in previous studies, are confirmed and described with additional details. The proximity of emission sites, both to the plasmapause layer and to the geomagnetic equator surface, seems to be of great importance in the behaviour of the $(n + 1/2)\, f_{ce}$ wave characteristics. Our study indicates for the first time, that both the intensity of $(n + 1/2)\, f_{ce}$ emissions, and the number of harmonic bands they cover, are increasing as the observation point is located further away outside from the plasmapause layer. Moreover, a study of the wave intensity in the first harmonic band (near $3/2\, f_{ce}$) shows higher amplitude for these emissions than previous published values, these emissions can play a role in the scattering of hot electrons. Finally, geomagnetic activity influence, studied via time series of the D_{st} index preceding observations, indicates that $(n + 1/2)\, f_{ce}$ emission events are observed at CLUSTER position under moderate geomagnetic activity conditions, no specific D_{st} time variation being required.

Keywords: Electron cyclotron harmonic waves; Plasmasphere; Diffuse aurora

1. Introduction

Electron cyclotron harmonic (ECH) waves of various types have been observed in space since the advent of in situ measurements: in the Earth magnetosphere (Kennel et al., 1970; Christiansen et al., 1978; Olsen et al., 1987; Usui et al., 1999), as well as in the vicinity of other planets (Kurth and Gurnett, 1991). These emissions have been also observed in plasma laboratory (Krafft et al., 1992). Classifications of terrestrial ECH waves have been proposed, according to the available coverage of observations offered by the different spacecraft and their instrumentation (Hubbard and Birmingham, 1978, on IMP 6; Gough et al., 1979, on GEOS 2). Main classification criteria are the intensity and the frequency range of the emissions. In parallel with observations, and sometimes in advance from those, a large number of theoretical studies have been produced, concerning both the generation mechanisms of ECH waves, and their effects on the magnetospheric electron population. Kennel and Ashour-Abdalla (1982) published a comprehensive review of possible causes and effects.

* Corresponding author.
E-mail address: mazouz@cnrs-orleans.fr (F. El-Lemdani Mazouz).

0273-1177/$34.00 © 2008 COSPAR. Published by Elsevier Ltd. All rights reserved.
doi:10.1016/j.asr.2008.06.007

In this paper, we present CLUSTER observations of one type of terrestrial ECH waves, namely intense $(n + 1/2)$ f_{ce} emissions, where f_{ce} is the local electron gyrofrequency, such as those which have been reported to be observed in the inner magnetosphere (radial distance below $\sim$12 R_E), strongly confined to the geomagnetic equator (Gough et al., 1981). An important possible effect of these intense emissions is to operate a pitch angle diffusion of plasmasheet keV-electrons, and consequently their precipitation into the auroral ionosphere (Kennel et al., 1970; Lyons, 1974). Further studies (Belmont et al., 1983; Fontaine et al., 1986) have questioned, without excluding it, the hypothesis of responsibility of $(n + 1/2)$ f_{ce} emissions to operate strong pitch angle diffusion. Other works address the same question. Roeder and Koons (1989), from a statistical study using SCATHA and AMPTE IRM plasma wave data, drove a conclusion in agreement with Belmont et al. (1983). They show that amounts of intense equatorial $(n + 1/2)$ f_{ce} emissions are grossly insufficient to account for the diffuse auroral precipitation by quasi-linear pitch angle diffusion. In contrast, Horne et al. (2003), analysing a weak substorm injection event, and exploring the effects of propagation in a non homogeneous medium, find out that ECH waves resonate with electrons over a wide range of energies (from hundred of eV to a few keV), producing probably the major contribution to diffuse auroral precipitation for this substrom event.

The first motivation to the present study is to complete the observational data sets accumulated from last century's spacecraft, with CLUSTER wave data, in order to possibly open a new discussion of the questioned hypothesis. The second motivation deals with the origin of the waves, rather than with their consequences. We mainly describe the context of occurrence and intensity variations of the CLUSTER observed $(n + 1/2) f_{ce}$ emissions on a statistical basis. We discuss also the possible role in the apparition of these emissions of cold to warm electrons density ratio, of gradient density and of free energy sources. We present in addition, from event studies, some details of the wave spectral signature collected with WHISPER instrument on board CLUSTER. Those signatures have been shown from theoretical studies to be of importance in the search of the generation mechanism. Let us precise that we exclude in this study the waves at and above the upper hybrid frequency f_{uh}, sometimes associated to the lower frequency range of ECH emissions, but of different nature according to the shape of Bernstein mode dispersion relation (Bernstein, 1958).

The observations of the multi-satellite CLUSTER mission offer a useful complement to observational data sets acquired in the past. One difficulty encountered by spacecraft with low or moderate inclination has been their tendency to sample the emissions of interest, strongly confined in magnetic latitude ($<\pm 2°$), in an uneven way (see Hubbard et al., 1979, for IMP6 view; Gough et al., 1981, for GEOS 1 and GEOS 2 view; Roeder and Koons, 1989, for SCATHA and AMPTE IRM view). Indeed, with spacecraft of high eccentricity, like IMP 6, the null magnetic latitude is often reached at an inconvenient radial distance, outside of the radial range of the emissions (which are confined not far outside the plasmasphere). With spacecraft of small eccentricity but low inclination (SCATHA, GEOS 2), the maximum wave intensity can sometimes be missed, or sampled at an unknown part of the orbit, due to fluctuations in an unknown way of the real instantaneous magnetic configuration. In contrast, the polar orbit of CLUSTER (Escoubet et al., 1997), crosses the geomagnetic equator clearly and quickly around perigee (near 4 R_E, with an orbital period of 57 h) during the years 2002–2004 (period analysed). This property, combined with the good time resolution of the instruments, allows to sort out orbits with or without equatorial $(n + 1/2)$ f_{ce} emissions and precisely measure their equatorial intensity. The counter part is a quite limited radial exploration (less than 0.5 R_E). The radial average position (around 4 R_E) is, however, most of the time close to the plasmasphere boundary layer region (Carpenter and Lemaire, 2004), not far from the inner edge of the plasmasheet electrons (Horwitz et al., 1986), i.e. where the phenomena of interest are taking place.

In this work, we show that the large majority of CLUSTER orbits are able to observe equatorial $(n + 1/2)$ f_{ce} emissions. Moreover, the orbit evolution during 1 year offers a complete and regular MLT sampling, repeated during the 3 years analysed. Another useful complement of CLUSTER data set is to offer a multipoint view, within a short-time separation (of order 1 h), of the same event at small radial separation. This reveals the important role of radial distance to sort out cases of multi-harmonic ECH emissions, at $(n + 1/2)$ f_{ce}, from cases of single harmonic (monotonic) ones, at 3/2 f_{ce} only.

The data analysed and presented in this study are a set of electric field frequency spectra measured near the equatorial plasmapause layer by the Wave of HIgh frequency and Sounder for Probing of Electron density by Relaxation (WHISPER) instrument (Décréau et al., 1997) on board the 4 CLUSTER spacecraft. WHISPER instrument enables the observation of various natural emissions in the plasmasphere region (Canu et al., 2001), in particular the $(n + 1/2)$ f_{ce} emissions (El-Lemdani Mazouz et al., 2006). We begin in Section 2 with a presentation and a discussion of the spectral properties of $(n + 1/2)$ f_{ce} emissions, via an event study. In Section 3, we present statistics over the 2002–2004 period. The occurrence rate of the equatorial $(n + 1/2)$ f_{ce} emissions and their MLT localization are studied and discussed, as well as the intensity of the first harmonic band of these waves. Finally, the time correlation of the apparition of these emissions with geomagnetic activity time variation is investigated via the D_{st} index. Section 4 summarizes the main findings from this study.

2. WHISPER observations of equatorial electron cyclotron harmonics

Before studying the statistical properties of the intense equatorial $(n + 1/2)$ f_{ce} emissions recorded on CLUSTER,

we briefly show typical signatures of natural emissions observed in the plasmasphere, using an event study. As mentioned above, the data analysed are electric field frequency spectra measured by the WHISPER instrument (Décréau et al., 1997, 2001) combined with the Electric Field and Wave (EFW) instrument (Gustafsson et al., 1997), the latter providing the sensors and antenna (a double sphere dipole), and the former the receiving and spectral analysis chain. In addition to the measurements of natural emissions, the WHISPER instrument yields a diagnosis of the plasma frequency f_p and of the gyrofrequency f_{ce} using a sounding technique. In the inner magnetosphere, where the plasma is significantly magnetized ($3 < f_p/f_{ce} < 10$), a careful analysis of the information contained in the frequency pattern of plasma resonances, triggered locally by the sounder, yields not only the total electron density, but also the density of the cold part of the electron population. As an example, the analysis of an event taken in the noon sector, close to perigee (Trotignon et al., 2003), indicates a cold component equal to about 95% of the total electron component in the plasmasphere, and to about only 60% in the region located just outside.

Natural waves measured by the WHISPER instrument are presented in Fig. 1 for a perigee pass on August 7th, 2003. A colour coded frequency–time spectrogram (left panel) displays the general wave behaviour along the orbit of the CLUSTER spacecraft, C4, and a frequency spectrum (right panel) shows detailed spectral features observed near the geomagnetic equator. From 06:15 to 10:00 UT, the CLUSTER constellation crosses the outer plasmasphere, at ~14 MLT, and between −55° and +55° magnetic latitude ($\mathrm{Lat_{SM}}$). The latitude and MLT values are calculated in Solar Magnetic (SM) coordinates, using the model of Tsyanenko and Stern (1996). The plasma frequency, plotted as a white solid line, rises and falls with time, reaching a maximal value of ~60 kHz near geomagnetic equator, crossed around 08:09 UT. The short increase of plasma frequency at 08:04 UT (before the equator crossing), from ~60 to ~70 kHz, indicates a short incursion earthward from a sharp plasmapause knee (or a local structure), located at an L shell of about 4.5 R_E. The otherwise smooth variation of the plasma frequency along the orbit is quasi identical for the four spacecraft. Since they are configured in this case in a small formation (200 km average spacecraft separation), and despite a constellation very elongated along the orbit near perigee, it is possible to evaluate spatial gradients of measured physical parameters (Darrouzet et al., 2006; De Keyser et al., 2007). The magnitude of the density gradient vector culminates near geomagnetic equator, reaching a value of about 0.05 $\mathrm{cm^{-3}}$/km (De Keyser et al., 2007). Its direction points there toward Earth, as expected for a regular plasmasphere shape, locally axi-symmetric.

Various types of natural emissions are observed during this plasmasphere crossing. We now briefly describe emissions related to the electron gyrofrequency f_{ce} (about 9.4 kHz at equator) and observed below the plasma frequency f_p. The first type of such waves is intense emissions observed near 08:05 UT, confined within a few degrees of magnetic latitude. These emissions are observed in a harmonic form at successive frequencies of, respectively, ~15, ~26, ~35 kHz and above, between harmonics of f_{ce}, and are thus identified as $(n + 1/2)\, f_{ce}$ emissions. They are also characterized by a large frequency bandwidth, defined as the full width at half the intensity maximum (FWHM). We will discuss this property further down in this section. The second type of natural emissions below f_p is an emission existing over a larger magnetic latitude interval, $\mathrm{Lat_{SM}}$ varying from −15° to 15°. This spectral feature is highlighted in the figure with a yellow arrow. This emission, well defined in frequency, with a narrow bandwidth (< 2 kHz), is observed exactly at $1.1\, f_{ce}$. The intensity of this emission is two order smaller than the intensity of the equatorial emissions. They are a common feature on

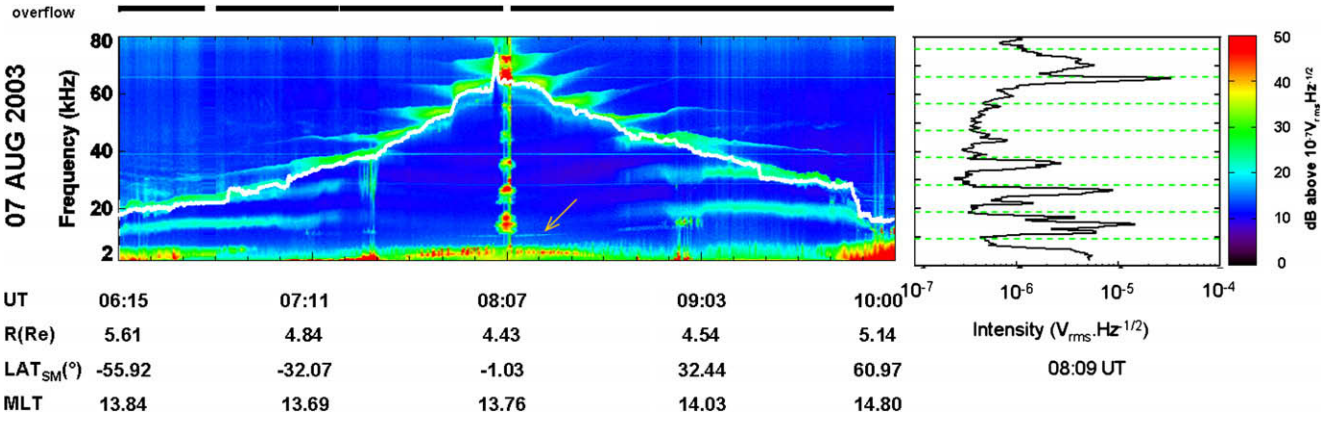

Fig. 1. Natural emissions measured on August 7th, 2003, by WHISPER on CLUSTER C4. (Left panel) Frequency–time spectrogram of the measured electric field. The white solid line follows the estimated plasma frequency. The arrow indicates emission at $1.1\, f_{ce}$. Coordinates of the satellite are given in Solar Magnetic (SM) coordinate system. The top bar indicates data status: white for data gaps, black for nominal conditions, green for data affected by saturation. (Right panel) Detailed spectrum at 08:09 UT, frequency band 0–80 kHz in ordinate. Dotted green lines indicate the electron gyrofrequency f_{ce} and its harmonics.

WHISPER spectrograms at perigee and can be associated or not with equatorial emissions. Other emissions displaying spectral feature related to f_{ce}, are observed both in the southern and in the northern hemisphere. Very faint (almost at noise level) in the equatorial region ($f_p > 30$ kHz and $|\mathrm{Lat_{SM}}| < 30°$), they reach significant levels further out the plasmasphere body, for long-time intervals (~1 h). The last type of emissions we can mention is observed below f_{ce} during several hours (from 07:00 to 10:00 UT). They are identified as chorus (Parrot et al., 2003).

In this work, we focus on the electrostatic emissions at $(n + 1/2)\, f_{ce}$ appearing within a few degrees of magnetic latitude. The right panel of Fig. 1 displays the frequency spectrum measured at 08:09 UT, just before the spacecraft crossed geomagnetic equator. We can clearly observe in this spectrum emissions, observed between two electron gyroharmonic frequencies, represented by green dotted lines on the figure. Four harmonic bands are observed, their intensity decreasing with the order of harmonic, from $1.7\ 10^{-5}\ V_{\mathrm{rms}}\,\mathrm{Hz}^{-1/2}$ for the first harmonic band to $8\ 10^{-7}\ V_{\mathrm{rms}}\,\mathrm{Hz}^{-1/2}$ for the fourth one. Note that the emission at the upper hybrid frequency f_{uh} (~65 kHz), is more intense ($> 5\ 10^{-5}\ V_{\mathrm{rms}}\,\mathrm{Hz}^{-1/2}$) than the $(n + 1/2)\, f_{ce}$ bands.

Some intense emissions can cause a saturation (overflow) of the instrument, leading to spurious frequency replicas. This is the case here around 08:08 UT as it is indicated in the figure by the green colour on the top bar of the spectrogram. However, despite the presence of these replicas, we are able to characterize properly the natural emissions at $(n + 1/2)\, f_{ce}$, because not all the spectra are affected.

The measured raw signal, S, is expressed in Fig. 1 in unity of $V_{\mathrm{rms}}\,\mathrm{Hz}^{-1/2}$, as is generally the case with WHISPER data. This quantity represents the electric field spectral density integrated along the effective length of the antenna, L_{eff}. Since the L_{eff} value depends significantly on the plasma regime considered and on the frequency range analysed (see Béghin et al., 2005, for a quantitative study of the behaviour of CLUSTER antennas), it is convenient to introduce this value only when necessary, i.e. when we need actual electric field values. This is the case here. In order to discuss possible contribution of $(n + 1/2)\, f_{ce}$ emissions to pitch angle diffusion, we must convert the WHISPER spectral density (in $V_{\mathrm{rms}}\,\mathrm{Hz}^{-1/2}$) to the amplitude (in $V_{\mathrm{rms}}\,\mathrm{m}^{-1}$, or $V\,\mathrm{m}^{-1}$ in short) of a sine electric field of equivalent energy. This allows a comparison with the threshold level, $E_0 \sim 1$ to $2\ \mathrm{mV\,m^{-1}}$, reported by several authors to cause pitch angle diffusion (see for example Belmont et al., 1983). The conversion reads:

$$E_{\sin\,\mathrm{e}}(V\mathrm{m}^{-1}) = \frac{\sqrt{\Delta F}(\mathrm{Hz})}{L_{\mathrm{eff}}(\mathrm{m})} S(V_{\mathrm{rms}}\mathrm{Hz}^{-1/2}) \qquad (1)$$

where ΔF is the useful frequency bandwidth.

L_{eff} is sometimes considered, for simplicity, to be equal to the actual tip to tip length of the antenna, 88 m in the case of CLUSTER. This would lead to an underestimation of the electric field value. We shall here adopt a more reasonable estimation, $L_{\mathrm{eff}} = 53$ m, valid for plasmas of 1–5 m Debye length, typical values in the outer plasmasphere (Décréau et al., 1982), in accordance with Fig. 6 of Béghin et al. (2005). Another factor of importance is the spin modulation coefficient, which affects the signal amplitude according to the antenna angle with magnetic field, since the $(n + 1/2)\, f_{ce}$ electric field is expected to be preferentially directed perpendicularly to magnetic field. As, near equator, the magnetic field makes a small angle with spin axis, we can ignore this effect in a first approximation. This could lead in any event to an underestimation of the electric field amplitude. Finally, we must evaluate the useful bandwidth ΔF. In the frame of theories involving monochromatic waves, we shall simply use the instrumental equivalent bandwidth, i.e. the $\Delta F = 556$ Hz value corresponding, in standard operation modes (324 Hz frequency resolution), to the conversion of a pure sine wave, leading finally to:

$$E_{\sin\,\mathrm{e}}(V\mathrm{m}^{-1}) = 0.44 S(V_{\mathrm{rms}}\mathrm{Hz}^{-1/2}) \qquad (2)$$

Eq. (2) might underestimate the meaningful amplitude estimation, since the observed bandwidth is generally higher, as described below.

The electrostatic emissions at $(n + 1/2)\, f_{ce}$ are observed between 08:04 UT and 08:10 UT with a total latitude extension of 4° in the modelled $\mathrm{Lat_{SM}}$ value (from −3° to +1°). The study of the overall frequency bandwidth of these emissions shows a maximum of the frequency bandwidth near geomagnetic equator, up to 8 kHz, with a higher value of the bandwidth for the first harmonic (the respective ratio of the bandwidth normalized to f_{ce} is ~80% for the first harmonic, 50% for the second one and 30% for the third one) in accordance with observations reported in previous works (Kennel and Ashour-Abdalla, 1982). Maximum values of intensity ($2.7 \times 10^{-5}\ V_{\mathrm{rms}}\,\mathrm{Hz}^{-1/2}$) and bandwidth are reached at 08:07 UT at modelled latitude $\mathrm{Lat_{SM}} = -1°$, which we believe is the actual geomagnetic equator.

We can also point out that the good frequency resolution of the WHISPER instrument (324 Hz in standard mode) allows the detection of interesting fine structures that are showing up in the detailed successive spectra recorded. For this event, if we focus on the 3/2 f_{ce} band: starting at 08:04 UT, it displays a double peak (f_{peak}/f_{ce} equal, respectively, to 1.5 and 1.7), which evolves into a triple peak (f_{peak}/f_{ce} equal, respectively, to 1.25, 1.52 and 1.76) at 08:09 UT, as shown in right panel of Fig. 1, at a less than 3° magnetic latitudinal distance. This evolution in the detailed structure of the 3/2 band is not explained by a change in the magnitude of the magnetic field which is constant (within less than 0.5%) between the two observations. Alternatively, if we focus on the evolution of the spectral pattern with the order of harmonic band considered, we can point out that the frequency of the maxima of intensity of each harmonic is shifted from the exact half of the bandwidth. This frequency increases from about 3/2 f_{ce} for the first harmonic band, to higher values in frequency for the

higher harmonics (5/2 f_{ce}, ...) up to 4.8 f_{ce} for the fourth harmonic band. Various positions in frequency could be explained by the different instability mechanisms leading to the apparition of these emissions, like a loss cone one for emissions lower than the exact half and a thermal anisotropy for the emissions higher than the exact half (Kennel and Ashour-Abdalla, 1982). Moreover, as shown by Horne et al. (2003), $(n + 1/2)f_{ce}$ waves are very sensible to propagation effects, which could explain some of the observed evolutions.

In summary, we show on this event study that $(n + 1/2)f_{ce}$ waves are strongly collimated near the geomagnetic equator. The ±2° latitudinal range is representative of all our observations. Another notable experimental result is the observation of fine structures inside the harmonic bands, with a complex evolution with respect to magnetic latitude. The evolution noted here is specific to the analysed event: other events show different behaviours, but most of them display fine frequency structures, which have not been, at this time, fully described (see Koons and Fennell, 1984; Paranicas et al., 1992, for examples of observed fine structures). It is outside the scope of this paper to discuss any interpretation, but we wish to underline the fact that a significant wave activity is present over a large part of the 3/2 f_{ce} harmonic band, as well as, in many cases, in the higher harmonic bands, as we will see in the next section.

3. Statistical study

In this part, we present a statistical study of $(n + 1/2)\,f_{ce}$ emissions. As mentioned before, we use WHISPER data collected by the CLUSTER spacecraft near perigee, over the years 2002–2004. At perigee (located around 4 R_E geocentric distance), we can monitor each crossing of the geomagnetic equator and check the presence of the emissions we are interested in. The 3 years duration of the data set analysed, compared to the orbital period duration (57 h), leads to a significant number of perigee passes (461 events), covering all MLT sectors.

During years 2002–2004, the average size of CLUSTER constellation varies from 100 to 6000 km. Because the constellation is elongated along the polar orbit at perigee, its projection onto the geomagnetic equator plane has a significantly smaller size: the maximal separation distances at equator crossings is always less than 0.5 R_E. Moreover, the crossings occur within 1 h at most. This delay is shorter than characteristic durations involved in global dynamics of the plasmasphere, i.e. in generation and corotation of a large plasmapause structure: such durations are typically higher than 3 h and less than 3 days (see for instance Pierrard and Cabrera, 2005). We can see that the four spacecraft will generally observe no major changes from the first to the last crossings at the same perigee pass, since they are grouped together in space and time. In contrast, changes in the plasmasphere between two successive perigee passes are expected. For our statistical study, we have chosen to treat data from a single satellite over a long period rather than to analyse observations from all spacecraft over a shorter period. We have selected the satellite CLUSTER 3 (C3). In this way, a database of 461 perigee events, which can be considered as statistically independent, has been constructed. All MLT sectors are equally covered.

3.1. Analysis of perigee data

The detection and characterization of $(n + 1/2)\,f_{ce}$ emissions near perigee have been performed by combining manual and automatic processing steps. In a first step, we have examined dynamic spectrograms near perigee, and have identified and listed the approximate times of geomagnetic equator crossings as indicated by a standard model of magnetic field. Our visual inspection allows distinguishing and listing perigee passes with or without $(n + 1/2)\,f_{ce}$ waves. It has been useful in particular to examine detailed spectrograms over passes when WHISPER saturation level is reached, in order to distinguish actual $(n + 1/2)\,f_{ce}$ events from frequency replica of the saturating signal. As we have seen in Section 2, this is possible as, generally, not all individual spectra are affected by saturation during perturbed perigee events, thus these events are taken into account in our statistics. Lastly, we note the number of harmonic bands displaying $(n + 1/2)\,f_{ce}$ emissions.

The series of approximate times at equator crossings, t_{in}, have been used as an input for a second processing step, which performs an automatic analysis of each event with waves. We make use of a tool, which localizes, in each individual WHISPER frequency spectrum, the most significant maxima of signal intensity (Rauch et al., 2006). Frequency peaks can then be followed over a given time and frequency interval. We have chosen to deal with a domain of 10 min time duration, centerd at t_{in}, and of 0.8 f_{ce} frequency width, centerd at 1.5 f_{ce}. Inside this time–frequency domain, the tool identifies and follows in time the peak of highest intensity. The gyrofrequency f_{ce} is derived for each spectrum from the magnetic field intensity measured by the FGM instrument (Balogh et al., 2001). The complete operation is repeated over higher electron gyroharmonic bands. The lowest frequency band, around 1.5 f_{ce}, is always present whenever higher harmonics are. A detailed analysis is conducted in this specific frequency band, whereby four quantities are calculated: the frequency and peak intensity of the main peak, its frequency bandwidth and its energy integrated over the frequency bandwidth. Their time variations are monitored over the 10-min interval. In practice, the peak is visible (i.e. above noise level) not over the whole duration of the time interval, but only over a part of it. We note the time and latitude at the two extrema (one in each hemisphere) between which the peak is visible. Finally, the time when the electric field amplitude reaches its maximal value determines the exact reference time of the event, t_{ref}.

Observations at perigee are sorted out according to three event groups.

- No data: WHISPER is not operational at the time of perigee crossing; 74 events (16% of the orbits) belong to this category.
- No $(n + 1/2)\ f_{ce}$ emissions present near geomagnetic equator; 123 events (27% of the orbits) belong to this category.
- $(n + 1/2)\ f_{ce}$ emissions present near geomagnetic equator; 264 events (57%) belong to this category. We can sort these equatorial events further, according to two subclasses, mono-harmonic ones (i. e. only $3/2\ f_{ce}$ waves) and multi-harmonic ones. Their relative proportion is, respectively, 18% and 82%.

We can note from this first analysis that the $(n + 1/2)\ f_{ce}$ waves are a common phenomenon in the equatorial region around the perigee altitude of CLUSTER, with a proportion of 68% of wave events among all crossings with data.

3.2. Latitudinal dependence

The analysis described above can be directly used to study the latitudinal dependence of the $(n + 1/2)\ f_{ce}$ emissions. First, we examine latitudes at the times of reference, t_{ref}. All 264 events of our database indicate a latitude, obtained with the Tsynanenko and Stern (1996) model, close to 0° (0.2° in average, with a standard deviation of 1.5°). Second, we examine the latitudinal extension of the events, evaluated from the first and last detection of the main peak (belonging to the lowest harmonic band). Those detections are, for all events, located inside the [−3°, +4°] latitude interval. Third, we examine how the frequency bandwidth Δf at half magnitude (FWHM) of the main peak of lowest harmonic band varies with latitude. This quantity reaches a maximum value near geomagnetic equator, and behaves similarly in higher harmonic bands: its largest value occurs at the same latitude than in the lowest band. In addition, the study of the ratios $\Delta f/f_{ce}$ indicates a typical value of 70% for the lowest harmonic band, and decreasing ratio values for higher harmonic bands. Lastly, we analyse the frequency position of the main peak emission, normalized to the local gyrofrequency value, f_{ce}. This parameter varies significantly with magnetic latitude, crudely symmetrically with respect to the true equator position (at maximal intensity). This behaviour could result from propagation in a spatially non homogenous medium.

In any case, the geomagnetic equator position appears to be of great importance in the detailed behavior of $(n + 1/2)\ f_{ce}$ waves.

3.3. Magnetic local time dependence

3.3.1. Wave occurrence versus MLT

We concentrate now on the C3 perigee passes with WHISPER data (387 passes), analysed as described above. The occurrence of $(n + 1/2)\ f_{ce}$ emissions as a function of the MLT sector is displayed in Fig. 2a. Twelve cells of dimension $1\ R_E \times 2$ h MLT are drawn in polar coordinates. In each cell, we show in colour code the number of passes with equatorial $(n + 1/2)\ f_{ce}$ emissions, divided by the number of C3 crossings (with data available). The cells are centered at 4 R_E, which is approximately the geocentric distance of C3 at the time of geomagnetic equator crossing. Precise positions in R-MLT at equator crossings are indicated by the white crosses and black circles corresponding respectively to crossings with or without waves. We note that the occurrence of the waves is significant, 40% or more, in all MLT sectors. CLUSTER's orbit configuration in years 2002–2004 appears thus to be suitable for a statistical study of those waves. Clearly, $(n + 1/2)f_{ce}$ emissions are observed with a higher probability in the dawn sector (03–09 MLT) than in average, and, in contrast, with a lower probability in the dusk sector (16–18 MLT). This result agrees with previous studies (Roeder and Koons, 1989; Christiansen et al., 1978). Moreover, such a dawn-dusk asymmetry looks roughly like that of the equatorial plasmapause, which leads us to study further a possible relationship between both phenomena. More precisely: are $(n + 1/2)\ f_{ce}$ emissions co-located with a plasmapause layer? How closely? To evaluate this, we need to estimate the distance between C3 and the plasmapause layer. After discussing the above results in view of a global empirical modelled plasmapause, we will use WHISPER proper measurements of equatorial densities, indicating where the spacecraft crosses the plasmasphere.

3.3.2. Evaluation of CLUSTER distance to plasmapause

The comparison of the position of C3 at perigee with Carpenter's empirical model of the plasmapause position (Carpenter, 1970), represented in the bottom right of Fig. 2a, shows that at the radial distance of 4 R_E, the spacecraft is close to the plasmapause on all MLT sectors except for the bulge (18–23 MLT). In this empirical model (based on ground based noise whistler signatures), the plasmapause is identified as a sharp knee in the density radial profile, the density jump going typically from 20 to 200 cm^{-3}. A significant part (20– 80 cm^{-3}) of this density jump corresponds to a plasma frequency band (40–80 kHz) within the WHISPER frequency range. Each plasmasphere crossing observed by WHISPER (near CLUSTER perigee) can be translated in a density profile versus radial distances above 4 R_E, and thus can be related to a modelled plasmapause knee. Some of those profiles indicate that the plasmasphere crossing includes the plasmapause knee, others that the knee is located below CLUSTER perigee. We can hence qualify the empirical position of the plasmapause in each pass by the value of the equatorial plasma frequency $f_{p\text{-}eq}$.

Values of $f_{p\text{-}eq}$ are obtained by visual inspection of WHISPER perigee spectrograms. This frequency is evaluated, near geomagnetic equator crossing, with a precision of ±5 kHz. One of the seven values (going from 30 to >80 kHz) is assigned: 30 kHz referring to actual $f_{p\text{-}eq}$ values between 25 and 35 kHz, 40 kHz to $f_{p\text{-}eq}$ values between 35 and 45 kHz and so on, 80 kHz to $f_{p\text{-}eq}$ values between 75 and 80 kHz. Finally, the value >80 kHz refers to cases of equatorial plasma frequencies above WHISPER limit.

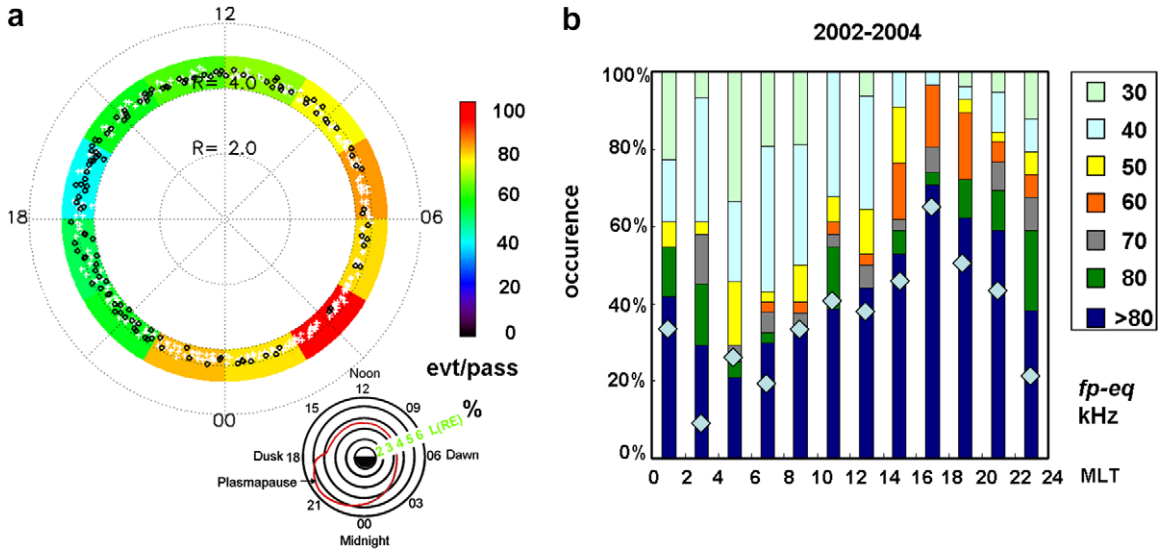

Fig. 2. Magnetic local time dependence. Panel (a) Occurrence of the $(n + 1/2)$ f_{ce} equatorial emissions in an R-MLT plane. Positions of geomagnetic equator crossings with or without observation of $(n + 1/2)$ f_{ce} emissions are represented, respectively, by white crosses and black circles. A modelled plasmapause position in the geomagnetic equatorial plane is presented in the bottom right corner (from Carpenter, 1970). Panel (b) Relative occurrence of equatorial plasma frequency values measured by WHISPER at geomagnetic equator crossings, in the different MLT sectors. Diamonds indicate the percentage of absence of $(n + 1/2)$ f_{ce} emissions at crossings.

To identify the plasmapause knee, we choose the critical values of $f_{p\text{-}eq} = 60$ kHz, equivalent to a density $N_e \sim 45\ cm^{-3}$, a value located in the middle part of the plasmapause density jump.

The variations of $f_{p\text{-}eq}$ estimated for the C3 plasmasphere crossings are represented on Fig. 2b as a function of the MLT sector. The relative number of cases in each class is represented by the length of colour bar assigned to each class. Those values cover a large range at all MLT sectors, the distribution being clearly MLT dependant. The occurrence of high plasmasphere densities varies according to the different MLT sector in a way directly related to the morphology of the average plasmapause shown, with a typical dawn-dusk asymmetry. When C3 is located beyond the modelled plasmapause (dawn and morning MLT sectors), $f_{p\text{-}eq}$ is then, with a high probability, lower than 60 kHz. When CLUSTER is located below the modelled plasmapause (bulge to midnight MLT sector), $f_{p\text{-}eq}$ is then, with a high probability, higher than 60 kHz.

We will now use the parameter $f_{p\text{-}eq}$ as a proxy of the distance to the plasmapause and we will sort and discuss the characteristics of $(n + 1/2)$ f_{ce} emissions (existence, intensity, number of harmonics) according to this parameter.

3.3.3. Wave occurrence versus distance to the plasmapause

We have recognized that both MLT and distance to the plasmapause might play a role on the emission of $(n + 1/2)f_{ce}$ waves. We compare now the MLT dependence of, first, the occurrence of the waves and, second, the distribution of the proxy $f_{p\text{-}eq}$. The proportion of equatorial crossings without emissions is shown in Fig. 2b for each MLT sector (light blue diamond). The MLT variation of this value follows quite well the proportion of $f_{p\text{-}eq} > 80$ kHz. This is not by pure chance. Actually, all non occurrence cases are observed under $f_{p\text{-}eq} > 80$ kHz conditions (or $f_{p\text{-}eq} = 80$ kHz, for a small number of them). We can also notice this feature in Table 1, where all values of low plasma frequency ($f_{p\text{-}eq} \leqslant 60$ kHz) correspond to crossings

Table 1
Occurrences of $(n + 1/2)$ f_{ce} emissions according to local time sectors established from 387 perigee passes with data

	Occurrence			$f_{p\text{-}eq} \leqslant 60$ khz				Intensity har1 $\geqslant 10^{-4} V_{rms}\ Hz^{-1/2}$		
	EQ (%)	3/2 (%)	Multi (%)	tot (%)	EQ (%)	3/2 (%)	Multi (%)	EQ (%)	3/2 (%)	Multi (%)
Dawn 03-09 MLT	81	7	74	60	60	0	60	70	0	70
Noon 09-15 MLT	64	9	55	48	48	2	46	51	2	49
Dusk 15-21 MLT	48	15	33	24	24	5	19	41	5	36
Midnight 21-03 MLT	77	19	58	38	38	0	38	59	0	59

Column "occurrence" :occurrence of passes with events "EQ", "3/2" and "multi" refer respectively to all $(n + 1/2)$ f_{ce} emissions, mono-harmonic emissions and multi-harmonic emissions.

Column "$f_{p\text{-}eq} \leqslant 60$ khz": occurrences of all passes under moderate equatorial plasma frequency conditions listed in the sub-column "tot" are compared to occurrences of passes combining moderate equatorial plasma frequency and observations of events of the tree types described above.

Column "intensity": occurrences of events with intense ($>10^{-4}$ $V_{rms}\ Hz^{-1/2}$) signal level in the first harmonic band listed according to the tree types of emissions described above.

with observations of $(n + 1/2)\, f_{ce}$ emissions in the different MLT sectors. Consequently, it seems that high equatorial densities, meaning that CLUSTER spacecraft is inward of the plasmapause layer, are unfavorable to $(n + 1/2)\, f_{ce}$ emissions. We can also observe that the $(n + 1/2)\, f_{ce}$ emissions are systematically observed for a large range of values of the equatorial plasma frequency, whatever MLT sector considered. More precisely, in the dawn sector we see that the high occurrence of the observations correspond to low values of the equatorial plasma frequency (CLUSTER outward the plasmapause layer) on most of the cases. In the bulge sector, the low occurrence of observations can be attributed to the high values of $f_{p\text{-}eq}$ prevailing in this region. Conversely, some cases with wave occurrence are observed under high plasma frequency conditions, i.e. inward of the plasmapause layer, especially in the night sector, as if the shielding of $(n + 1/2)\, f_{ce}$ emissions by high densities would be less efficient in the night sector. This behavior could be explained by the higher occurrence of small and local density structures in this part of the outer plasmasphere (Darrouzet et al., 2004). An event study has indeed shown that density depletions actually favor this type of emissions. Another possible explanation is that this MLT sector is crudely co-located with the plasmasheet injection boundary of electrons (Horwitz et al., 1986), possibly associated to $(n + 1/2)\, f_{ce}$ emissions.

3.4. Spectral properties versus equatorial densities

The number of harmonics observed by WHISPER for the $(n + 1/2)\, f_{ce}$ emissions varies from one to nine, with a higher proportion of multi-harmonic observations (82% of the total number of equatorial observations). Monotonic (single harmonic) emissions are observed with different proportions according to the MLT sector considered. The highest ratio of monotonic observations versus multi-harmonic observations is found in the dusk sector and the lowest ratio is found in the dawn sector (see Table 1).

A detailed statistical analysis of the monotonic emission events indicates that their presence is regulated by the radial distance to plasmapause (defined by the $f_{p\text{-}eq}$ parameter proxy). All observations fit with the following scenario: an observer, moving from the inner plasmasphere toward the outer region, would first find no equatorial emissions (in the inner plasmapause layer, i.e. at $f_{p\text{-}eq} \geqslant 80$ kHz), then monotonic ones ($f_{p\text{-}eq}$ at intermediate values) then multi-harmonic ones ($f_{p\text{-}eq}$ at low values). Indeed, statistically, higher is the value of $f_{p\text{-}eq}$, lower is the value of the number of harmonics observed. As shown in Table 1, the proportion of $f_{p\text{-}eq} \leqslant 60$ kHz is no more than 5% for mono-harmonic emissions, whereas it is 60% for multi-harmonic ones. We can also notice that all plasmasphere crossings at values of $f_{p\text{-}eq} \leqslant 60$ kHz are associated with observations of equatorial events, in most cases of multi-harmonic emissions.

Furthermore, using event studies, El-Lemdani Mazouz et al. (2006) have compared observations from the four spacecraft located at small geocentric distance from each other. They show that radial distance to plasmapause is indeed a strict regulator of the number of harmonic bands displaying $(n + 1/2)\, f_{ce}$ waves: higher is the radial distance (lower is the $f_{p\text{-}eq}$ value), higher is the upper n value of the series, within the limit $(n + 1/2)\, f_{ce} < f_{p\text{-}eq}$. This finding can be interpreted by considering that the ratio of warm to cold electron plasma populations is an important factor of the generation mechanism. This ratio increases with radial distance, as the ionospheric plasma source is progressively supplemented by plasmasheet source, thus favoring the apparition of a higher number of harmonics.

3.5. Intensity analysis

One of the drivers for studying the intensity of the $(n + 1/2)\, f_{ce}$ emissions is the question mentioned in the introduction section, related to the origin of diffuse auroras: are emissions sufficiently intense to cause particle precipitations? In order to examine the situation from CLUSTER point of view, we have performed a statistical analysis of the measured wave intensity level in the first harmonic band (generally the most intense one).

To this end, we detect automatically, for each event, the time and frequency of the main peak of intensity in the first harmonic band, and record its intensity level. The normalized histogram shown in Fig. 3a displays the distribution of intensities characterizing the events, as a function of the MLT sector of observation. We divide the intensity levels in five ranges, going from 1.10^{-7} to $1.10^{-1} V_{\mathrm{rms}}\,\mathrm{Hz}^{-1/2}$. The proportion of events with intensity higher than $10^{-4}\ V_{\mathrm{rms}}\,\mathrm{Hz}^{-1/2}$ is around 57% of the total observed equatorial events. The most intense emissions are present in the dawn sector, where the maximum amount of events with high intensity levels ($I \geqslant 10^{-4}\ V_{\mathrm{rms}}\,\mathrm{Hz}^{-1/2}$) is about 70% of the total number of events detected in this sector. The less intense emissions are present in the dusk sector, with a relative number of events with $\mathrm{I} \geqslant 10^{-4}\ V_{\mathrm{rms}}\,\mathrm{Hz}^{-1/2}$ amounting to about 41%. We can note that a high proportion of intense emissions corresponds to a high occurrence of the events (shown in Fig. 2a).

We can relate the intensity levels of events with the equatorial plasma frequency value, by analyzing in parallel Figs. 2b and 3a. The proportion of events with $I \geqslant 10^{-4}\ V_{\mathrm{rms}}\,\mathrm{Hz}^{-1/2}$ increases with the proportion of $f_{p\text{-}eq} \leqslant 60$ kHz in all MLT sectors. Globally, the scatter plot of intensity values versus the $f_{_{p\text{-}eq}}$ parameter, displayed in Fig. 3b, indicates a clear anti-correlation between the two quantities of interest, as if the intensity would increase with the geocentric distance of observation (which globally increases as $f_{p\text{-}eq}$ decreases). Furthermore, case events analysis of multipoint measurements at large spacecraft separation indicates, systematically, the same behavior (see El-Lemdani Mazouz et al., 2006): in a given MLT sector and under given geophysical conditions, the intensity of equatorial ECH emissions increases with geocentric distance. In paral-

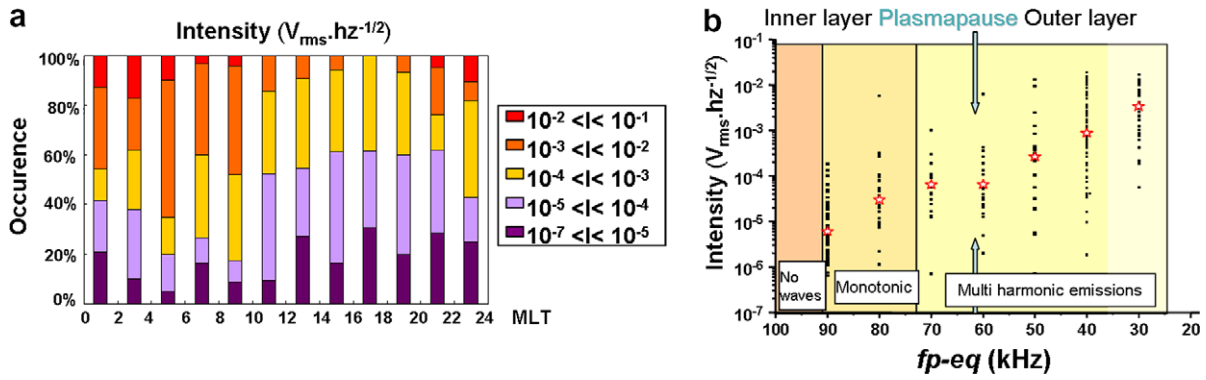

Fig. 3. Analysis of wave intensity. Panel (a) MLT distribution of wave intensities (expressed as the spectral density of a potential difference) at peak of equatorial 3/2 f_{ce} emissions. Panel (b) Distribution of electric field intensities in the different classes of equatorial plasma frequency. Red stars indicate median values. Three different background colours underline three plasma frequency domains in which typical spectral behaviors are encountered, as labelled at the bottom of the figure.

lel, the number of harmonic bands with emissions increases.

Fig. 3b shows a large dispersion in intensity values obtained for each assigned value of the equatorial plasma frequency. This is likely due to different behaviors according to the MLT sector concerned. Compared occurrences of large intensities and low equatorial plasma frequencies versus MLT sectors are summarized in Table 1. When we compare dawn and dusk MLT sectors, or dawn and noon MLT sectors, the occurrence of large intensities increases with the occurrence of low plasma frequencies (as in the general behavior shown in Fig. 3b). An exception appears when we compare noon and midnight sectors, as the occurrence of intensities at $I \geqslant 10^{-4}\ V_{\rm rms}\,{\rm Hz}^{-1/2}$ increases from 51% (noon sector) to 59% (midnight sector), whereas the occurrence of $f_{p\text{-}eq} \leqslant 60$ kHz decreases from 48% to 38%. Lastly, Table 1 indicates that the first harmonic band is more intense for multi-harmonic observations than for monotonic ones, the proportion of intense monotonic emissions being no more than 2% of the total emissions of high intensity ($I \geqslant 10^{-4}\ V_{\rm rms}\,{\rm Hz}^{-1/2}$). The highest occurrence of intense monotonic observations is observed in the dusk sector.

Thus, we can say that the proximity to the plasmapause position plays a role in governing the intensity of the waves, with an exception in the midnight sector. Such a behavior could be due to a comparatively higher density ratio of warm to cold populations in the sector populated by the plasmasheet source. The WHISPER sounder is able to estimate this ratio (Trotignon et al., 2003), but a statistical study of this quantity as a function of MLT sector and equatorial density is yet to be done.

Finally, we compare intensities of 3/2 f_{ce} emissions estimated from the GEOS perspective (Belmont et al., 1983) with intensities obtained from the CLUSTER perspective. The estimation of reference for GEOS is given in Fig. 2 of Belmont et al. (1983), i.e. "the typical wave amplitude of 1 mV.m^{-1} was exceeded during 15% of time". The latter figure is obtained at $L = 6.6$, a magnetic latitude of 0°, in the night side MLT sector (22–6), assuming a 1 kHz wave bandwidth. The conversion indicated in Eq. (2) leads to an intensity expressed in WHISPER units of $I = 2.25\ 10^{-3}\ V_{\rm rms}\,{\rm Hz}^{-1/2}$ being equivalent to 1 mV m^{-1}, considering in this case a ~0.5 kHz bandwidth, a figure corresponding to monochromatic waves. Taking account of the difference in geocentric distances (the minimum wave amplitude goes as $L^{-1/2}$), the minimum intensity of reference is finally $\sim 3\ 10^{-3}\ V_{\rm rms}\,{\rm Hz}^{-1/2}$, a threshold exceeded in about 32% of the night side observed events. This result indicates that the intense 3/2 f_{ce} ($I \geqslant 3\ 10^{-3}\ V_{\rm rms}\,{\rm Hz}^{-1/2}$) emissions are observed with higher proportions during CLUSTER perigee passes in the night side sector comparing to GEOS and SCATHA statistical studies. This proportion is still insufficient to explain the scattering of hot electrons, in the frame of theories implying monochromatic waves, where higher proportions of intense emissions are required (Lyons, 1974).

However, the large spectral width of $(n + 1/2)\ f_{ce}$ emissions observed in practice (~5 kHz) would increase this proportion up to more than 50% of the night side events indicating that they could indeed play a role in the generation of diffuse auroras.

3.6. Geomagnetic activity influence

In order to study the correlation between the geomagnetic activity and the presence of the equatorial emissions, we analyse the $D_{\rm st}$ index, characterizing the intensity of the ring current, associated to observations. Values of $D_{\rm st}$ are followed in reverse chronology between the time of geomagnetic equator crossing up to 24 h before. The reason behind this proceeding is the following: the plasmasphere response to a geomagnetic disturbance is quasi instantaneous in the night sector, but happens with several hours delay in the dayside, since corotation has to propagate the deformation from the night to noon sector (Décréau et al., 1982; Pierrard and Cabrera, 2005). A delay of 24 h is thus a reasonable time interval to follow up variations of $D_{\rm st}$ in correlation with observations. We define four different classes of activity, each referring to a given $D_{\rm st}$ range,

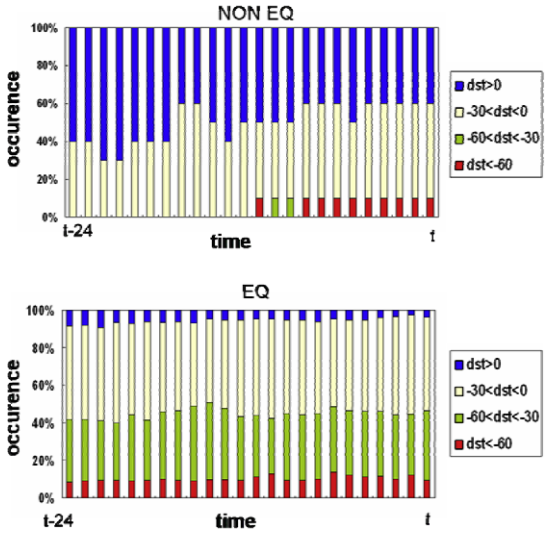

Fig. 4. Role of geomagnetic activity. Time evolution of D_{st} index associated with the absence (top) or presence (bottom) of waves at $(n+1/2)\,f_{ce}$.

from quiet geomagnetic activity to disturbed geomagnetic activity. The histograms plotted in Fig. 4 display the relative occurrence of each D_{st} class measured in each of the 24 one hour time intervals preceding the observation. The variation of class occurrences with respect to time delays is shown respectively for equator crossings when we see equatorial emissions, called EQ (bottom panel), and for the crossings without equatorial emissions, called non EQ (top panel). We can note that EQ events are observed during low or moderate geomagnetic conditions ($-60 < D_{st} < 0$), whereas non EQ events are observed during quiet to low activity conditions ($-30 < D_{st}$). The distribution over the different activity classes is stable with time delays, except for the non event cases, which displays a higher proportion of quiet conditions for longest delays. The difference in geomagnetic conditions prevailing respectively for non events and for events can be interpreted as follow. Non events are preceded by a relatively long period of quiet conditions. It is known that under such situation, the plasmasphere expands towards distances significantly larger than CLUSTER geocentric distance at equator. Such situation will drive high equatorial plasma frequencies, screening the waves (Section 3.3.3). On the other hand, our analysis shows that EQ events do not require any specific D_{st} time variation, like for instance a substorm onset, to be triggered. They are observed during a variety of conditions, mostly moderate and likely stable, similar conditions than those which prevail during diffuse auroras.

4. Summary and conclusion

The observations described and analysed here are made with the WHISPER instrument on board the CLUSTER constellation, when the spacecraft cross the magnetic equator at its perigee, i.e. at a geocentric distance of about 4 R_E. The value of the plasma frequency, $f_{p\text{-}eq}$, measured at geomagnetic equator crossings indicates if the plasmapause boundary is located inward ($f_{p\text{-}eq} > 60$ kHz) or outward ($f_{p\text{-}eq} \leqslant 60$ kHz) of the crossing position, and how deep inside or far outside of the plasmapause the satellites are. Statistically, it yields a qualitative estimation of the distance between the observation and the plasmapause boundary. The CLUSTER orbit gives a good MLT sampling and a clear localization of the geomagnetic equator, in contrast with previous studies, affected by gaps in the MLT sector coverage or in the latitude coverage. A 3 years long observational period has permitted to conduct a meaningful statistical analysis of the properties of $(n+1/2)\,f_{ce}$ emissions in function of magnetic latitude, MLT sector and, for the first time, of qualitative distance to the plasmapause boundary. The main results obtained from this study can be listed as follows:

(1) WHISPER instrument detects $(n+1/2)\,f_{ce}$ emissions on all CLUSTER geomagnetic equator crossings, whatever MLT sector considered, under the condition that the crossing occurs in the outer plasmasphere region. Quantitatively, a proportion of 68% of all perigee passes is associated with $(n+1/2)\,f_{ce}$ events, the condition $f_{p\text{-}eq} \leqslant 60$ kHz insuring that emissions are present. Such a phenomenon seems thus to be a permanent feature of the outer plasmasphere region, not restricted to any given MLT sector.

(2) The latitudinal extension of the phenomenon, evaluated from measurements of the main emission, i.e. near $3/2\,f_{ce}$, does not vary much from event to event. This extension, defined by the southern and northern limits of a measurable emission intensity level (at or above a threshold of $2\ 10^{-7}\ V_{rms}\ Hz^{-1/2}$) stays within the $[-3°$ to $4°]$ magnetic latitude interval.

(3) The number of electron cyclotron harmonic bands where $(n+1/2)\,f_{ce}$ emissions are present is governed by the way CLUSTER crosses the plasmasphere. It increases with the radial distance of observation, from zero (no emission) deep inside the plasmasphere, up to several bands in the outermost part of the geomagnetic equator surface explored by CLUSTER. The single band case is generally observed just inside of a plasmapause layer. In addition, the intensity of $(n+1/2)\,f_{ce}$ emissions is generally decreasing with the order of the band considered.

(4) The intensity in the main band (near $3/2\,f_{ce}$) is increasing with the radial distance of observation (Fig. 3b). Quantitatively, the median value of the intensity increases from $6\ 10^{-6}\ V_{rms}\ Hz^{-1/2}$ within the plasmasphere (when $f_{p\text{-}eq}$ is above WHISPER's frequency range) by more than two order of magnitudes higher, i.e. up to $3\ 10^{-3}\ V_{rms}\ Hz^{-1/2}$ for the class of events corresponding to the outermost region ($f_{p\text{-}eq} = 30$ kHz).

(5) The MLT sector of observation has a significant influence on the occurrence of $(n+1/2)\,f_{ce}$ emissions (Fig. 2a), as reported in the past. Quantitatively, the

percentage of geomagnetic equator crossings with wave events observed from CLUSTER varies from 90% in the 02–04 MLT sector down to 35% in the 16–18 MLT sector. Such behaviour is mainly the consequence of the non axi-symmetric shape of the plasmapause boundary, observed here from a fixed radial distance perspective. This affects the MLT distribution of cases placed respectively on each side of the plasmapause, hence, according to (3), the distribution of events and non events. Nevertheless, the MLT sector exerts a proper influence on wave events: almost no wave events are seen in the dayside when $f_{p\text{-}eq}$ is above WHISPER's frequency range, whereas a significant number of them is seen under the same conditions in the night sector. Event studies have shown that fine density structures, present in this MLT sector, favour the $(n + 1/2)\, f_{ce}$ emissions.

(6) The MLT sector of observation has a significant influence on the intensity of the $3/2 f_{ce}$ emission (Fig. 3a). It is not easy to disentangle both influences, of MLT proper and of distance to plasmapause, on the intensity, since the distribution of the $f_{p\text{-}eq}$ parameter values measured during wave events displays a dawn – dusk asymmetry (Fig. 2b) similar to the one displayed by the distribution of the wave intensity values (Fig. 3a). However, some facts indicate that MLT has an influence of its own: (i) the occurrence of intensities at $I \geqslant 10^{-4}\ V_{\mathrm{rms}}\ \mathrm{Hz}^{-1/2}$ increases from noon to midnight sector, when at the same time the occurrence of $f_{p\text{-}eq} \leqslant 60$ kHz decreases; (ii) the highest occurrence of intense monotonic observations corresponds to the dusk sector.

(7) Lastly, the influence of geomagnetic activity on the presence of emissions is studied via the variation of the D_{st} index. Results show that the $(n + 1/2)\, f_{ce}$ emissions are observed during periods of moderate and stable activity, similar to those prevailing during diffuse auroras.

It is important to add that the multipoint capability of the CLUSTER mission has been significant in order to test our statistical results concerning the influence of the distance to plasmapause. Data sets of four spacecraft, crossing the geomagnetic equator surface at short distances from each other, and within a short-time delay, have been compared. Multipoint event studies have been able to confirm the fine role of geocentric distance, revealed for the first time by our study, both on the number of electron cyclotron harmonic bands displaying emissions, and on the wave intensity in the main band.

Concerning the question of the intensity of the emissions leading to pitch angle diffusion, WHISPER measurements show that the highest intensities of the $(n + 1/2)\, f_{ce}$ emissions are localized in the dawn sector. Our evaluation of the percentage of CLUSTER wave events exceeding the threshold referred to as necessary to drive a significant pitch angle diffusion is 32%, a factor two higher than what has been measured from GEOS 2 perspective (Belmont et al., 1983). This fact, combined with the clear increasing of intensity with distance to plasmapause (Fig. 3b) indicates that the 'hottest' region (where the ECH wave intensity is the highest) might be located in between radial distances of CLUSTER perigee and of GEOS 2, and could be indeed sufficient to create diffuse auroras. Further studies, including a larger CLUSTER data set and other data sets (about plasmasheet injections, other geomagnetic activity indices, diffuse aurora observations), could help to conclude.

Regarding to which generation mechanism is the source of $(n + 1/2)\, f_{ce}$ emissions, the limited study described here provides a few indications: (i) the emissions are not generated in a plasma regime including the single dense cold electron population prevailing in the inner plasmasphere; (ii) the exact position in frequency of the peak in intensity varies within each harmonic band; (iii) it varies in addition with geomagnetic latitude, together with intensity variation; (iv) specific behaviours are observed, according to which event is analysed. A fine analysis of wave features, associated to the context found in each event, and to wave level estimations, could help to shed a new light on this question.

Acknowledgements

We thank the teams at ESOC (Darmstadt, Germany), JSOC (Oxford, UK) and Department of automatic control and systems engineering, University of Sheffield (UK) for their constant support of CLUSTER operations. We want also to thank the FGM team (Imperial College, UK) for providing magnetic field data.

References

Balogh, A., Carr, C.M., Acuña, M.H., et al. The Cluster magnetic field investigation: overview of in-flight performance and initial results. Ann. Geophys. 19, 1207–1217, 2001.

Béghin, C., Décréau, P.M.E., Pickett, J., et al. Modeling of CLUSTER's electric antennas in space: application to plasma diagnostics. Radio Sci. 40, 1–18, 2005.

Belmont, G., Fontaine, D., Canu, P. Are equatorial electron cyclotron waves responsible for diffusive auroral electron precipitation? J. Geophys. Res. 88, 9163–9170, 1983.

Bernstein, I.B. Waves in a plasma in a magnetic field. Phys. Rev. 109, 10–21, 1958.

Canu, P., Décréau, P.M.E., Trotignon, J.G., et al. Identification of natural plasma emissions observed close to the plasmapause by the Cluster-Whisper relaxation sounder. Ann. Geophys. 19, 1697–1709, 2001.

Carpenter, D.L. Whistler evidence of the dynamic behavior of the duskside bulge in the plasmasphere. J. Geophys. Res. 75, 3837–3847, 1970.

Carpenter, D.L., Lemaire, J. The plasmasphere boundary layer. Ann. Geophys. 22, 4291–4298, 2004.

Christiansen, P.J., Gough, M.P., Martelli, G., et al. GEOS-1 observations of electrostatic waves and their relationship with plasma parameters. Space Sci. Rev. 22, 383–400, 1978.

Darrouzet, F., Décréau, P.M.E., De Keyser, J., et al. Density structures inside the plasmasphere: cluster observations. Ann. Geophys. 22, 2577–2585, 2004.

Darrouzet, F., De Keyser, J., Décréau, P.M.E., et al. Spatial gradients in the plasmasphere from cluster. Geophys. Res. Let. 33, L08105, 2006.

De Keyser, J., Darrouzet, F., Dunlop, M.W., et al. Least-square gradient calculation from multi-point observations of scalar and vector fields: methodology and applications with cluster in the plasmasphere. Ann. Geophys. 25, 971–987, 2007.

Décréau, P.M.E., Béghin, C., Parrot, M. Global characteristics of the cold plasma in the equatorial plasmapause region, as deduced from the GEOS 1 Mutual Impedance Experiment. J. Geophys. Res. 87, 695–712, 1982.

Décréau, P.M.E., Fergeau, P., Krasnoselskikh, V., et al. Whisper, a resonance sounder and wave analyser: performances and perspectives for the CLUSTER mission. Space Sci. Rev. 79, 157–193, 1997.

Décréau, P.M.E., Fergeau, P., Krasnoselskikh, V., et al. Early results from the Whisper instrument on CLUSTER: an overview. Ann. Geophys. 19, 1241–1258, 2001.

El-Lemdani Mazouz, F., Grimald, S., Rauch, J.L., et al. Electrostatic and electromagnetic emissions near the plasmasphere. A case event: 27 May 2003, in: Proceedings of the Cluster and Double Star Symposium – 5th Anniversary of Cluster in Space, Noordwijk, The Netherlands, 19–23 September 2005, ESA SP-598, 2006.

Escoubet, C.P., Russell, C.T., Schmidt, R. The Cluster and Phoenix Missions. Kluwer Academic Publishers, Dordrecht, The Netherlands, 658 pp., 1997.

Fontaine, D., Perraut, S., Cornilleau-Wehrlin, N., et al. Coordinated observations of electron energy spectra and electrostatic cyclotron waves during diffuse auroras. Ann. Geophys. 4, 405–412, 1986.

Gough, M.P., Christiansen, P.J., Martelli, G., et al. Interaction of electrostatic waves with warm electrons at the geomagnetic equator. Nature 279, 515–517, 1979.

Gough, M.P., Christiansen, P.J., Gershuny, E.J.E.S. Wave morphology near the geostationary orbit. Adv. Space Res. 1, 337–343, 1981.

Gustafsson, G., Boström, R., Holback, B., et al. The electric field and wave experiment for the Cluster mission. Space Sci. Rev. 79, 137–156, 1997.

Horne, R.B., Thorne, R.M., Meredith, N.P., et al. Diffuse auroral electron scattering by electron cyclotron harmonics and whistler mode waves during an isolated substorm. J. Geophys. Res. 108, 1290–1302, 2003.

Horwitz, J.L., Menteer, S., Turnley, J., et al. Plasma boundaries in the inner magnetosphere. J. Geophys. Res. 91, 8861–8882, 1986.

Hubbard, R.F., Birmingham, T.J. Electrostatic emissions between electron gyroharmonics in the outer magnetosphere. J. Geophys. Res. 83, 4837–4850, 1978.

Hubbard, R.F., Birmingham, T.J., Hones Jr., E.W. Magnetospheric electrostatic emissions and cold plasma densities. J. Geophys. Res. 84, 5828–5838, 1979.

Kennel, C.F., Scarf, F.V., Fredricks, R.W., et al. VLF electric field observations in the magnetosphere. J. Geophys. Res. 75, 6136–6149, 1970.

Kennel, C.F. and Ashour-Abdalla, M. Electrostatic waves and the strong diffusion of magnetospheric electrons. In Magnetospheric plasma physics edited by A. Nishida, 245 pp., D. Reidel, Hingham, Mass., 1982.

Koons, H.C., Fennell, J.F. Fine structure in electrostatic emission bands between electron gyrofrequency harmonics (from magnetospheric observations). J. Geophys. Res. 89, 3015–3018, 1984.

Krafft, C., Matthieussent, G., Thevenet, P., et al. Simultaneous emissions at $n\omega c$ and $(n + 1/2)\omega c$ in space and laboratory plasmas. J. Geophys. Res. 97, 14977–14987, 1992.

Kurth, W.S., Gurnett, D.A. Plasma waves in planetary magnetospheres. J. Geophys. Res. 96, 18977–18991, 1991.

Lyons, L.R. Electron diffusion driven by magnetospheric electrostatic waves. J. Geophys. Res. 79, 575–580, 1974.

Olsen, R.C., Shawhan, S.D., Gallagher, D.L., et al. Plasma observations at the Earth's magnetic equator. J. Geophys. Res. 92, 2385–2407, 1987.

Paranicas, C., Hughes, W.J., Singer, H.J., et al. Banded electrostatic emissions observed by the CRRES plasma wave experiment. J. Geophys. Res. 97, 13889–13898, 1992.

Parrot, M., Santolik, O., Cornilleau-Wehrlin, N., et al. Source location of chorus emissions observed by Cluster. Ann. Geophys. 21, 473–480, 2003.

Pierrard, V., Cabrera, J. Comparison between EUV/IMAGE observations and numerical simulations of the plasmapause formation. Ann. Geophys. 23, 2635–2646, 2005.

Rauch, J.L., Suraud, X., Décréau, P.M.E., et al. Automatic determination of the plasma frequency using image processing on whisper data, in: Proceedings of the Cluster and Double Star Symposium – 5th Anniversary of Cluster in Space, Noordwijk, The Netherlands, 19-23 September 2005, ESA SP-598, 2006.

Roeder, J.L., Koons, H.C. Survey of electron cyclotron waves in the magnetosphere and the diffuse auroral electron precipitation. J. Geophys. Res. 94, 2529–2541, 1989.

Trotignon, J.G., Décréau, P.M.E., Rauch, J.L., et al. The whisper relaxation sounder onboard cluster: a powerful tool for space plasma diagnosis around the Earth. Cosmic Res. 41 (4), 369–372, 2003.

Tsynanenko, N.A., Stern, D.P. Modeling the global field of the large-scale Birkeland current system. J. Geophys. Res. 101, 27187–27198, 1996.

Usui, H., Matsumoto, H., Mukai, T., et al. GEOTAIL observation of electron cyclotron harmonic waves near the dayside magnetopause. Adv. Space Res. 24, 99–102, 1999.